Performance Characterization of Polarimetric Active Radar Calibrators and a New Single Antenna Design

Kamal Sarabandi, *Member, IEEE*, Yisok Oh, *Student Member, IEEE*, and Fawwaz T. Ulaby, *Fellow, IEEE*

Abstract—**A polarimetric active radar calibrator (PARC) is a high radar-cross-section transponder with a known scattering matrix. This paper deals with three PARC-related topics. The first involves experimental measurements of the magnitudes and phases of the scattering-matrix elements of a pair of PARC's that operate at 1.25 GHz and 5.3 GHz. The measurements, which were obtained by a polarimetric scatterometer calibrated using a recently developed single-target-calibration technique (STCT), were conducted over a wide range of incidence angles (relative to the boresight direction) in the azimuth, elevation, 45°, and 135° planes. The 5.3 GHz PARC, which consisted of two antennas placed several wavelengths apart, exhibited symmetrical patterns with no ripples and excellent isolation between orthogonal polarization channels. In contrast, the 1.25 GHz PARC, whose antennas were in very close proximity of one another, exhibited unsymmetrical patterns as well as ripples in the phase patterns, thereby introducing errors in the elements of the scattering matrix. To avoid this problem, the antennas should be placed several wavelengths apart. Alternatively, a single-antenna PARC can be designed using an orthomode transducer. The design, construction, and performance evaluation of such a PARC is the second topic discussed in this paper, and the third topic pertains to extending STCT so it may be applied equally well using a PARC rather than being limited to using reciprocal passive calibration devices such as spheres and trihedral corner reflectors.**

I. Introduction

POLARIMETRIC imaging SAR has been shown to be an important remote sensing tool for the acquisition of quantitative information about the earth's environment. To make effective utilization of its data, it is necessary to calibrate the radar system by measuring its response to one or more calibration devices with known scattering matrices. Calibration targets can be categorized into two major groups: (a) passive calibrators; and (b) active calibrators [1]. Although passive calibrators are more stable and reliable than their active counterparts, they are less desirable because of their large physical dimensions. Another desirable feature of an active radar calibrator is that its location in an image and its SAR response (spread function) can be manipulated. For example, by inserting a delay-line between the receiver and transmitter of a PARC, its image can be located on a dark background, hence yielding a better signal to background ratio [4], [5]. Also the spread function of a PARC can be controlled by modulating the radar signal passing through the PARC [2]. In recent years, polarimetric active radar calibrators (PARC) have been used extensively, and current plans call for their use for external calibration of SAR systems [3] in support of future spaceborne missions.

The success of external calibration relies on the knowledge of the scattering matrix of the calibration target(s). Also, from a practical point of view, the scattering matrix of a calibration target must be rather insensitive to orientation angles. Although it may be possible to estimate the elements of the scattering matrix for a calibration target to a reasonable extent, manufacturing tolerances may leave a fair amount of uncertainty in the estimated values. Therefore it is imperative to measure the calibrators against a precise calibration target (such as a metallic sphere) under laboratory condition. This also reveals another drawback of passive calibrators with large physical dimensions, namely that the far-field condition and uniform illumination criteria are difficult to meet in the laboratory.

Until recently, it has been very difficult to measure the scattering matrices of targets, with the desired accuracy, over a wide range of incidence angle and frequency. Advances in technology and calibration methods have made it possible to measure the elements of the scattering matrix with an accuracy of 0.5 dB in magnitude and 5° in phase [7]. The first part of this paper presents measurements of the scattering patterns of L- and C-band PARC's, which are currently being used by JPL in support of its airborne polarimetric SAR program. The measurements were performed in the University of Michigan's anechoic chamber using a fully automated polarimetric scatterometer [8]. The scatterometer system is itself calibrated using a single-target-calibration technique (STCT) [7] based on a four-part network model. As originally developed, STCT required the use of a reciprocal passive calibration target. By way of extending STCT so it may be used with a PARC instead, a new formulation is presented in Section IV.

One of the observations noted from the measurements performed on the L-band (1.25 GHz) and C-band (5.3 GHz) PARC's is that the backscattering patterns of the

Manuscript received March 14, 1991; revised January 13, 1992. This work was supported by the Jet Propulsion Laboratory under contract JPL-C-958749.

The authors are with the Radiation Laboratory, Department of Electrical Engineering and Computer Science, The University of Michigan, Ann Arbor, MI 48109-2122

IEEE Log Number 9204924.

magnitude can exhibit asymmetry and the phase patterns may include ripples if the PARC's two antennas are in close proximity of one another. To avoid wide physical separation between the two antennas, the manufacturer of the L-band PARC had constructed the unit with the two antennas placed next to one another. To avoid the proximity problem, while simultaneously avoiding the inconvenience of having to place the two antennas some distance from each other as well as ensuring that each is properly oriented towards the radar, which is particularly a problem in field deployments in support of calibrating an airborne or spaceborne SAR, a new single-antenna PARC with high radar cross section has been designed and tested. Measurements characterizing its performance are given in Section V.

II. Measurement System Configuration

Polarimetric measurements of PARC's were performed using L- and C-band scatterometers. A simplified block diagram of the scatterometer system is shown in Fig. 1. The scatterometer is an HP 8753A-based system with both phase and magnitude measurement capability and 100 dB of dynamic range. The ability of the network analyzer to generate the time domain response of the frequency measurement allows us to separate unwanted short-range signals from the desired target response (known as software gating). The sequence of polarization selection, data collection, and target orientation is performed via an HP 9000 series computer. The relay actuator energizes the frequency and polarization switches. The amplifier and pulsing network eliminates the short-range returns from the antenna and circulators, thereby increasing the dynamic range available for RCS measurements [6]. With this scheme, the receiver is switched off during transmission and then reconnected when the target return is expected to arrive at the receiver. Since the switching is performed at a much higher rate than the receiver's bandwidth, the network analyzer does not sense that the incoming signal is pulsed and it is measured as if it were a CW signal.

Because a PARC has a high gain amplifier, reflections from nearby objects might increase the feedback between its two antennas, thereby causing internal oscillation. To avoid this problem, and also to have a very good signal to background ratio, the PARC's were mounted on a Styrofoam ® pedestal in an anechoic chamber. The correct position of the PARC's with respect to the antenna coordinate system was accomplished by an azimuth-over-elevation positioner. The azimuth turntable is driven by a computer-controlled stepper motor with an accuracy of a fraction of a tenth of a degree, and the elevation controller is a precise analog positioner.

To calibrate the PARC's, we used the single-target calibration technique (STCT) described in [7]. The error associated with the measurement of the scattering matrix using this technique is less than 0.5 dB in magnitude and 5° in phase. With the STCT, the antenna cross-talk contamination and channel imbalances are obtained by measuring the response of only a single calibration target, namely a metallic sphere. This technique is immune to errors caused by target alignment with respect to the antenna coordinate system.

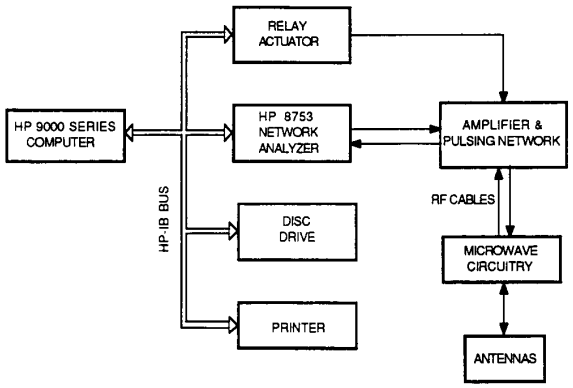

Fig. 1. Block diagram of the scatterometer system.

Applying the four-port network approach [7] to a polarimetric radar with similar v and h antennas, it is shown that the measured scattering matrix of a target with scattering matrix **s** can be obtained from

$$\mathbf{M} = \begin{bmatrix} R_1 & 0 \\ 0 & R_2 \end{bmatrix} \begin{bmatrix} 1 & C \\ C & 1 \end{bmatrix} \mathbf{s} \begin{bmatrix} 1 & C \\ C & 1 \end{bmatrix} \begin{bmatrix} T_1 & 0 \\ 0 & T_2 \end{bmatrix} + \mathbf{N} \quad (1)$$

where the **R** and **T** matrices account for the receive and transmit channel imbalances, C is the antenna cross-talk contamination factor, and **N** is a matrix representing thermal noise and background reflections. It is worth noting that if the v and h antennas of the radar system are not similar, then two different cross-talk factors C_1 and C_2 must be used in (1) instead. The background contribution **N** can be obtained by measuring the empty chamber and then subtracting from **M**, the effect of thermal noise can be minimized by an integration process.

Denoting the measured scattering matrix elements of the sphere and the PARC by, respectively, m_{ij}^0 and m_{ij}^u, the unknown scattering matrix elements of the PARC can be obtained from the expressions

$$s_{vv} = \frac{1}{(1-C^2)^2} \cdot \left[-2C^2 \left(\frac{m_{12}^u}{m_{12}^0} + \frac{m_{21}^u}{m_{21}^0} \right) + (1+C^2) \left(\frac{m_{11}^u}{m_{11}^0} + C^2 \frac{m_{22}^u}{m_{22}^0} \right) \right] s^0$$

$$s_{hh} = \frac{1}{(1-C^2)^2} \cdot \left[-2C^2 \left(\frac{m_{12}^u}{m_{12}^0} + \frac{m_{21}^u}{m_{21}^0} \right) \right.$$

$$+(1+C^2)\left(\frac{m_{22}^u}{m_{22}^0}+C^2\frac{m_{11}^u}{m_{11}^0}\right)\Bigg]s^0$$

$$s_{vh}=\frac{C}{(1-C^2)^2}\cdot\left[2\frac{m_{12}^u}{m_{12}^0}+2C^2\frac{m_{21}^u}{m_{21}^0}-(1+C^2)\left(\frac{m_{11}^u}{m_{11}^0}+\frac{m_{22}^u}{m_{22}^0}\right)\right]s^0$$

$$s_{hv}=\frac{C}{(1-C^2)^2}\cdot\left[2\frac{m_{21}^u}{m_{21}^0}+2C^2\frac{m_{12}^u}{m_{12}^0}-(1+C^2)\left(\frac{m_{11}^u}{m_{11}^0}+\frac{m_{22}^u}{m_{22}^0}\right)\right]s^0$$

where s^0 is the theoretical value for the diagonal elements of the sphere's scattering matrix. The cross-talk contamination factor is given by

$$C=\pm\frac{1}{\sqrt{a}}(1-\sqrt{1-a})$$

where $a \triangleq (m_{12}^0 m_{21}^0/m_{11}^0 m_{22}^0)$ and the branch of the square root is chosen such that $\mathrm{Re}[\sqrt{1-a}]>0$. The uncertainty in the sign of C can be removed when measuring PARC's because the general trends of the relative phases of the scattering elements are known.

III. Experimental Results

The measurements reported in this section were performed in a 14-m-long anechoic chamber. The PARC under test was mounted on a styrofoam pedestal on an azimuth-over-elevation positioner. To ensure that the PARC is operating properly, the energy flow between the receive and transmit antennas was monitored by inserting a 20-dB directional coupler between the amplifier and the transmit antenna. Also, to avoid saturating the PARC's amplifier and the scatterometer receiver, the scatterometer transmit power was adjusted such that the PARC output power was about 5 dBm. For the actual radar-cross-section (RCS) measurements, the directional coupler was removed.

A 30-cm metallic sphere was used as the calibration target, and the signal to noise ratio was better than 30 dB in all cases. The L- and C-band measurements were performed over the following frequency ranges: 1.1–1.4 GHz and 5–5.5 GHz, respectively. All the data presented in this paper correspond to measurements at the center frequencies, namely 1.25 GHz for L-band and 5.3 GHz for C-band. Angular patterns of the radar cross section were measured over the range of incidence angle from $-40°$ to $+40°$, relative to the boresight direction, in the azimuth, elevation, 45°, and 135° planes.

The radar cross section of a PARC can be decomposed into two components. The first component is the contribution of the front panel and the antennas (passive contribution) and the second component is the contribution of the delay line and amplifier. Using the range-gating capability of the scatterometers, the two responses can be separated in time. In Fig. 2, which shows the time-domain response of an L-band PARC, it is easy to see that the component due to the passive contribution is at least 25 dB lower than the active component. Even so, in all of the results shown in this paper, the contribution due to the front panel and antennas has been gated out.

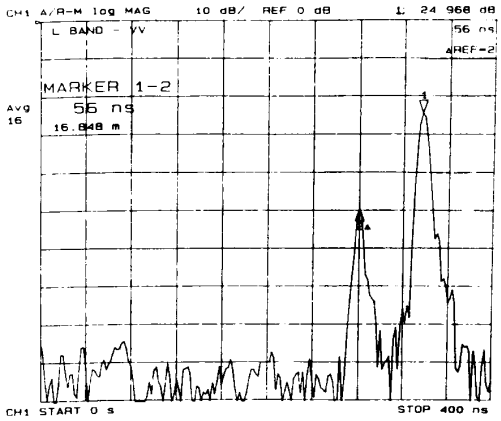

Fig. 2. Time domain response of an L-band PARC.

In this study three L-band and three C-band PARC's were measured. The results were basically the same among each set of three; hence we will present results for only one PARC at each band. In order to measure the RCS patterns in the desired planes, the PARC's were oriented as shown in Fig. 3.

The measured scattering patterns of the L- and C-band PARC's are shown in Figs. 4 and 5. The C-band patterns seem reasonable in the sense that the magnitude and the phase patterns are smooth and very close to the expected values; in Fig. 5(b), in the phase differences $\phi_{hh}-\phi_{vv}$ and $\phi_{hv}-\phi_{vv}$ are each $\simeq 180°$ and $\phi_{vh}-\phi_{vv}\simeq 0$. However, the L-band patterns in Fig. 4 are not quite symmetrical; the maximum RCS appears at about 10° from boresight in Fig. 4(a) and the measured phase patterns [Fig. 4(c)] are quite different from the expected behavior, both in level and angular variation (ripple effect). These problems are due to the fact that the transmit and receive antennas are very close to each other (almost touching). The antennas are in the near field of each other, causing the magnitude and phase patterns to have ripples and to be different from the patterns of isolated antennas. This was shown by separating the L-band antennas by two wavelengths, which led to much better performance.

IV. A Calibration Technique Using PARC's

Calibration of polarimetric space-borne imaging SAR requires calibration targets with very large radar cross section and PARC's seem to be the only logical choice. The scattering matrix of an ideal PARC comprised of orthogonally polarized transmit and receive antennas (Fig.

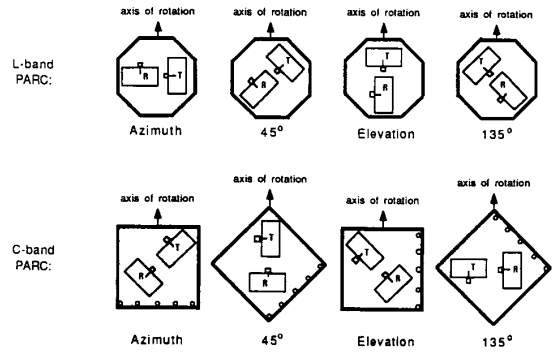

Fig. 3. The orientation of L- and C-band PARC's for pattern measurement.

3) has the following form

$$\mathbf{s}_p = \frac{1}{4}\sqrt{\frac{\sigma}{\pi}}\begin{bmatrix} -\sin 2\alpha & 1+\cos 2\alpha \\ 1-\cos 2\alpha & \sin 2\alpha \end{bmatrix}$$

where α is a rotation angle about the incidence direction and σ is the radar cross section of the PARC at $\alpha = 0$ (defined here to correspond to a vertically polarized transmit antenna and horizontally polarized receive antenna). Distortion parameters of a polarimetric radar usually are obtained by measuring a set of calibration targets with known scattering matrices. In general the distortion parameters are expressed in terms of transmit and receive distortion matrices, and the measured scattering matrix $\mathbf{M}$, ignoring noise effects, is related to the actual scattering matrix of the target $\mathbf{s}$ by

$$\mathbf{M} = \mathbf{RsT}. \tag{2}$$

Each calibration target provides four equations for the unknowns. This is not the case when a PARC is used as a calibration target because its scattering matrix is nonreciprocal and singular, that is $|\mathbf{s}| = |\mathbf{M}| = 0$. Hence, the single target calibration technique (STCT) cannot be applied directly because a PARC provides only three equations instead of four. To calibrate a polarimetric radar, at least two PARC's with independent scattering matrices are needed (different rotation angles α_1 and α_2). Applying the error model given by (1) to a radar system with possibly dissimilar v and h antennas, the measured scattering matrix of a target with scattering matrix $\mathbf{s}$ can be obtained from

$$\mathbf{M} = \begin{bmatrix} R_1 & 0 \\ 0 & R_2 \end{bmatrix}\begin{bmatrix} 1 & C_1 \\ C_2 & 1 \end{bmatrix}\mathbf{s}_p\begin{bmatrix} 1 & C_2 \\ C_1 & 1 \end{bmatrix}\begin{bmatrix} T_1 & 0 \\ 0 & T_2 \end{bmatrix}. \tag{3}$$

Since the radar cross section of a PARC is very large, the noise matrix $\mathbf{N}$ is ignored in (3). If the measured scattering matrix of PARC's 1 and 2 are denoted by $\mathbf{M}^1$ and $\mathbf{M}^2$ respectively, then

$$R_1T_1 = \frac{M^i_{11}}{(C_1^2-1)\sin 2\alpha_i + 2C_1} \tag{4}$$

$$R_1T_2 = \frac{M^i_{12}}{(C_1-C_2)\sin 2\alpha_i + (1-C_1C_2)\cos 2\alpha_i + 1 + C_1C_2} \tag{5}$$

$$R_2T_1 = \frac{M^i_{21}}{(C_1-C_2)\sin 2\alpha_i - (1-C_1C_2)\cos 2\alpha_i + 1 + C_1C_2} \tag{6}$$

$$R_2T_2 = \frac{M^i_{22}}{(C_2^2-1)\sin 2\alpha_i + 2C_2} \tag{7}$$

with $i = 1, 2$. The cross-talk factors can be obtained by eliminating the channel imbalances from the two measurements. For example, R_1T_1 and R_2T_2 from (4) and (7) can be eliminated to get

$$C_i = \frac{M^1_{ii} - M^2_{ii}}{M^2_{ii}\sin 2\psi_1 - M^1_{ii}\sin 2\psi_2} \pm \sqrt{\left(\frac{M^1_{ii} - M^2_{ii}}{M^2_{ii}\sin 2\psi_1 - M^1_{ii}\sin 2\psi_2}\right)^2 + 1} \tag{8}$$

where the sign of the square root is chosen such that $|C_i| \ll 1$. With C_1 and C_2 determined, the scattering matrix $\mathbf{s}$ of an unknown target with measured scattering matrix $\mathbf{M}^u$ can be calculated from

$$\mathbf{s} = \frac{1}{(1-C_1C_2)^2}\begin{bmatrix} 1 & -C_1 \\ -C_2 & 1 \end{bmatrix}\begin{bmatrix} \dfrac{M^u_{11}}{R_1T_1} & \dfrac{M^u_{12}}{R_1T_2} \\ \dfrac{M^u_{21}}{R_2T_1} & \dfrac{M^u_{22}}{R_2T_2} \end{bmatrix}\cdot\begin{bmatrix} 1 & -C_2 \\ -C_1 & 1 \end{bmatrix}. \tag{9}$$

V. Single-Antenna PARC

In this section, we discuss the design and measured performance of a wide-band high-RCS single-antenna PARC, which avoids the near-field problems discussed in Section III.

The theoretical radar cross section of an ARC is given by

$$\sigma = G_{\text{loop}}\frac{G_tG_r\lambda^2}{4\pi} \tag{10}$$

where G_t and G_r are the transmit and receive antenna gains, G_{loop} is the loop gain including amplifier gain and delay line and other RF circuit losses. To design an ARC with high RCS, we can either increase the loop gain or the

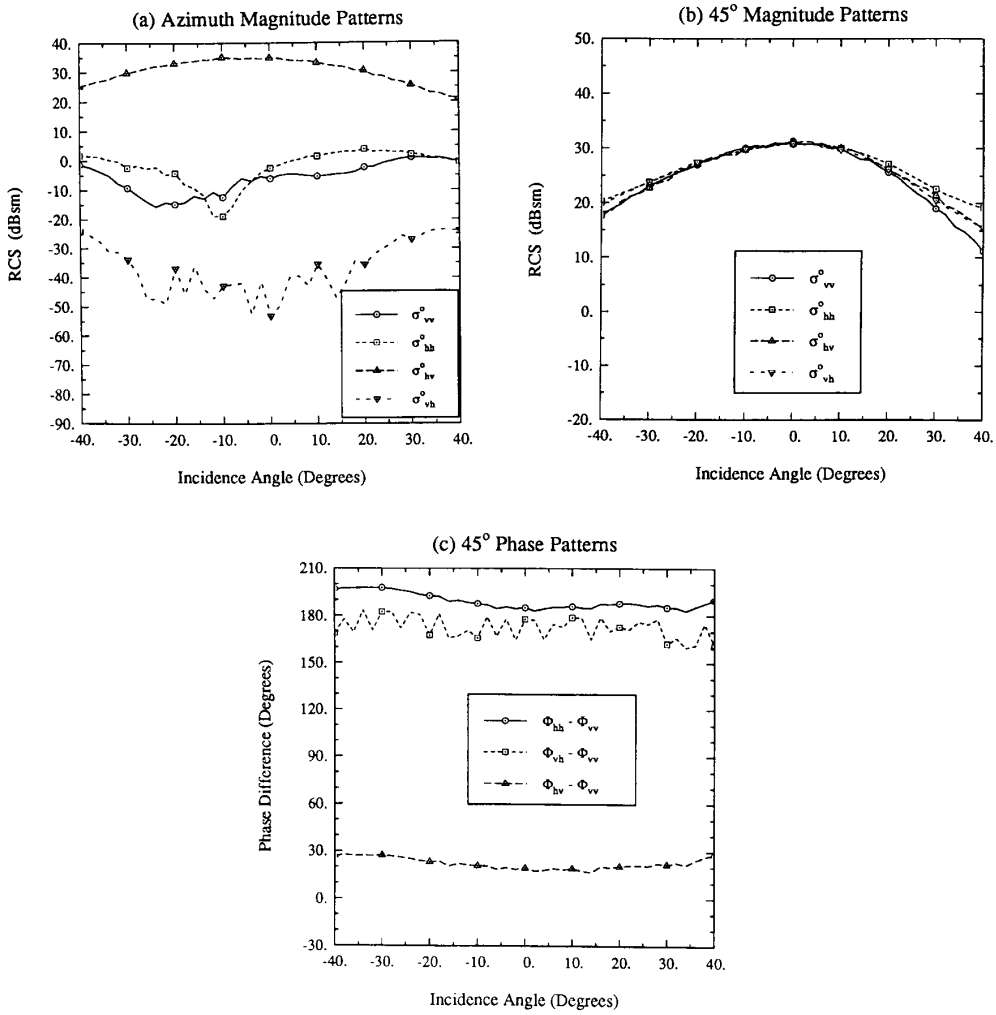

Fig. 4. Measured patterns for the L-band PARC.

antenna gains or both. The loop gain is limited by two factors: (a) the isolation between the receiver and transmitter; and (b) the amplifier stability requirements. The antenna gain is also limited by two factors: (a) beamwidth requirement; and (b) size and weight limitations. At low frequencies size and weight considerations become the dominant limiting factors.

To avoid the problems that occur when the transmit antenna is in close proximity of the receive antenna, which includes pattern asymmetry and magnitude and phase ripple, the antennas must be kept outside of the near-field zone of each other. If we increase the antenna gain, we further increase its far-field distance. Hence to use antennas with maximum allowable gain, we may have to mount the transmit and receive antennas on two separate panels. This has been the common practice at low frequencies (L- and P-band). Having transmit and receive antennas on separate panels causes difficulties in field deployment and uncertainty in the relative orientations of the antennas with respect to each other.

To circumvent the size and weight limitations and the problems associated with proximity, while simultaneously using the maximum allowable gain for the antennas, we propose a single antenna PARC (SAPARC). SAPARC uses a dual-polarized antenna with very good isolation between the polarization channels. One of the channels is used for reception and the other one is used for transmission. A block diagram of SAPARC is shown in Fig. 6. To obtain wide bandwidth and high cross-polarization isolation over the entire beamwidth, a square horn with a waveguide orthomode transducer (OMT) can be used. The detailed design steps of the OMT are outside the scope of this paper; however, we will briefly describe the main features and the overall performance of the antenna assembly. In order to reduce RF mismatch and cross-talk generation, the horn antenna was flared at three equally

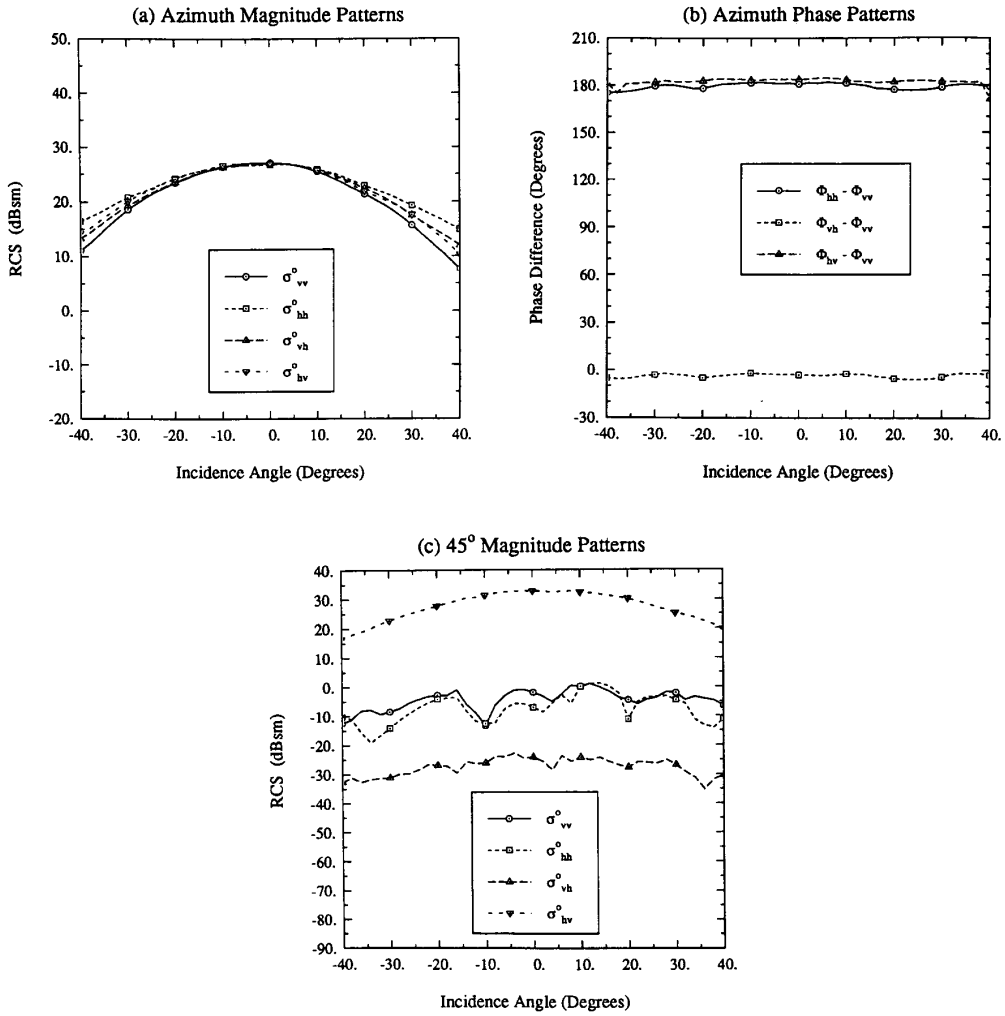

Fig. 5. Measured patterns for the *C*-band PARC.

spaced locations. The polarization separation is realized in a square *T*-junction using wire grids. The positions of the wires are chosen such that the return loss and cross talk are minimum. Fig. 7 shows the OMT and the square horn antenna.

A prototype SAPARC was constructed for operation over the 1.1–1.4 GHz. The overall isolation of the antenna and the OMT was measured to be better than 35 dB. The return loss of the OMT for both ports is better than -18 dB and the return loss of the antenna is better than -20 dB over the entire frequency band. If this structure is employed in a PARC configuration as shown in Fig. 6, a maximum of 55 dB in loop gain (stable condition) can be used. Therefore, for an antenna with aperture size 56 × 56cm, $(G^2\lambda^2/4\pi) \approx 11$ dB and a maximum radar cross section of 66 dBsm can be achieved. Fig. 8 shows measured angular patterns of a SAPARC designed with a moderate loop gain of 36 dB and an overall RCS of 47 dBsm. Fig. 8(a) and (b) show that the RCS

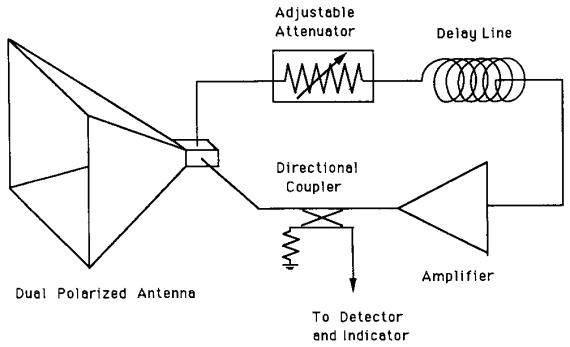

Fig. 6. Block diagram of a single antenna PARC.

patterns of the SAPARC are symmetrical and smooth, and the 3-dB beamwidth is about 17°, which is sufficient for most practical cases. The overall polarization isolation of the designed OMT and the antenna can be inspected

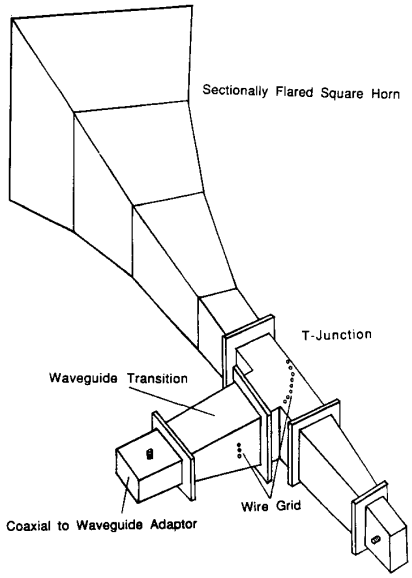

Fig. 7. Antenna assembly of the *L*-band SAPARC.

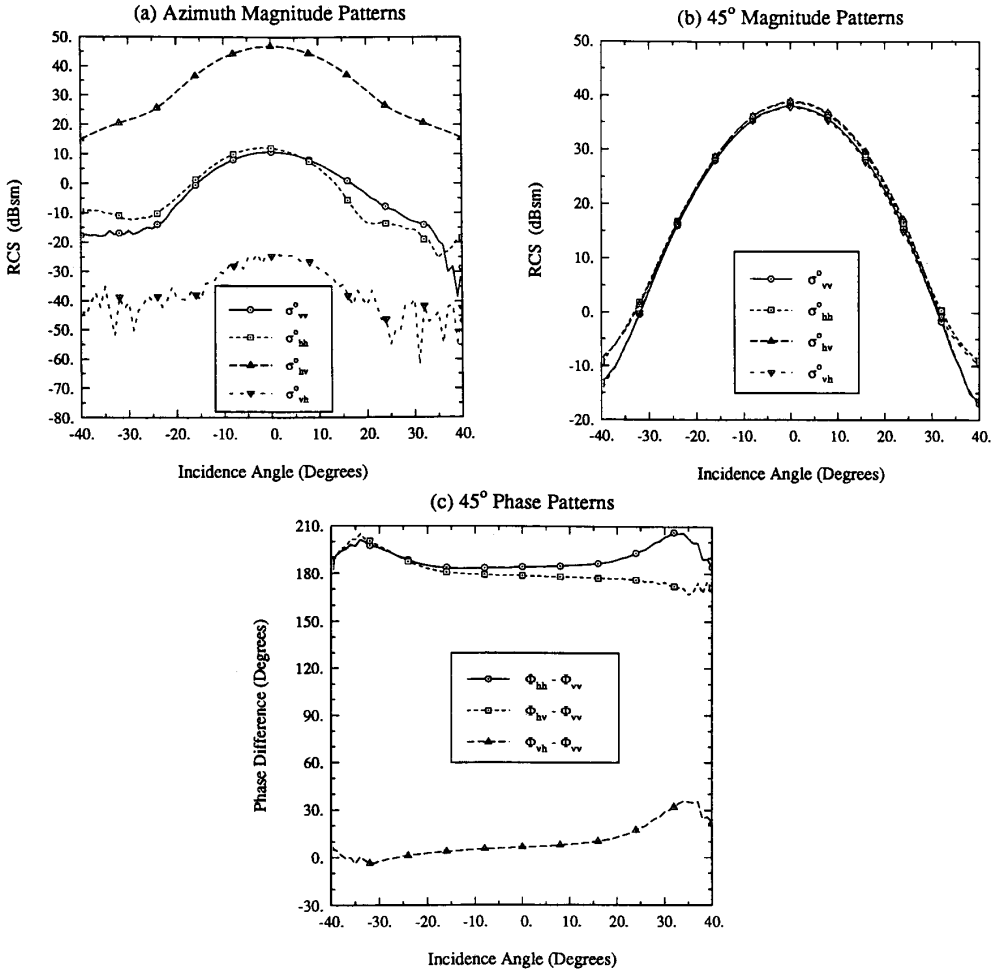

Fig. 8. Measured patterns for *L*-band SAPARC.

from Fig. 8(a) by comparing σ_{vh} to σ_{hh}. Noting that the uncertainty in phase measurement is about 5°, the measured phases of the scattering matrix elements of the SAPARC are very close to the expected values, as shown in Fig. 8(c).

VI. Conclusions

This paper discusses several topics associated with the use of PARC's to calibrate polarimetric radar systems. A calibration method that uses two PARC's in conjunction with the STCT is introduced. RCS patterns measured as a function of incidence angle are presented for *L*- and *C*-band PARC's at each of two different orientation angles. The measurements show that the RCS is not very sensitive to changes in the azimuth and elevation angles, but it is very sensitive to the rotation angle about the boresight direction. It is found that when the transmit and receive antennas of a PARC are, respectively, parallel and perpendicular to the vertical direction, small errors in the orientation angle or phase-measurement errors have a minor effect on calibration accuracy.

The measurements also show that when the antennas are in close proximity of one another, the RCS pattern becomes asymmetrical and ripples are observed in both the magnitude and phase patterns. To circumvent these problems, a single-antenna PARC design is introduced, along with measured patterns of a prototype model.

References

[1] D. R. Brunfeldt and F. T. Ulaby, "Active calibrators for radar calibration," *IEEE Trans. Geosci. Remote Sensing*, vol. 22, no. 2, 1984.

[2] D. R. Brunfeldt, "SAR response to modulated targets," in *Proc. IEEE Geosci. Remote Sensing Symp.*, Vancouver, July 1989.

[3] A. Freeman, Y. Shen, and C. L. Werner, "Polarimetric SAR calibration experiment using active radar calibrators," *IEEE Trans. Geosci. Remote Sensing*, vol. 28, no. 2, 1990.

[4] K. Komiyama, "Delayed-action reflector for external calibration of synthetic aperture radar," *Electronic Letters*, vol. 25, no. 7, pp. 468–470, Mar. 1989.

[5] K. Komiyama, Y. Kato, and I. Yokoshima, "Relocatable imaging using a delayed-action radar calibrator for SAR calibration," in *Proc. 1989 Int. Symp. Noise Clutter Rejection Radar Imaging Sensors*, pp. 717–721.

[6] V. V. Liepa, K. Sarabandi, and M. A. Tassoudji, "A pulsed network analyzer based scatterometer," *Proc. IEEE Geosci. Remote Sens. Symp.*, Vancouver, July 1989.

[7] K. Sarabandi and F. T. Ulaby, "A convenient technique for polarimetric calibration of radar systems," *IEEE Trans. Geosci. Remote Sensing*, vol. 28, no. 6, Nov. 1990.

[8] M. A. Tassoudji, K. Sarabandi, and F. T. Ulaby, "Design consideration and implementation of the LCX polarimetric scatterometer (POLARSCAT)," The University of Michigan, Radiation Laboratory Report No. 022486-T-2, June 1989.

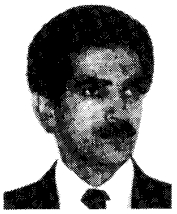

Kamal Sarabandi (S'87–M'90) was born in Tehran, Iran on November 4, 1956. He received the B.S. degree in electrical engineering from Sharif University of Technology, Tehran, Iran, in 1980; and the M.S.E. and Ph.D. degrees in electrical engineering in 1986 and 1989, respectively, as well as the M.S. degree in mathematics in 1989, all from the University of Michigan.

From 1980 to 1984 he worked as a microwave engineer in the Telecommunication Research Center in Iran. He is presently an Assistant Professor in the Department of Electrical Engineering and Computer Science at the University of Michigan. His research interests include electromagnetic scattering, microwave remote sensing, and calibration of polarimetric SAR systems.

Dr. Sarabandi is a member of the Electromagnetics Academy and USNC/URSI Cimmission F.

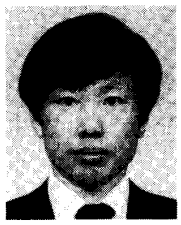

Yisok Oh (S'88) received the B.S. degree in electrical engineering from Yonsei University, Seoul, Korea, in 1982, and the M.S. degree in electrical engineering from the University of Missouri, Rolla, in 1988. He is currently working toward the Ph.D. degree in electrical engineering at the University of Michigan, Ann Arbor.

Currently he is a research assistant with the Radiation Laboratory, University of Michigan. His research interests include microwave remote sensing, with an emphasis on the interface between experimental measurements and theoretical models for electromagnetic wave scattering from earth terrain.

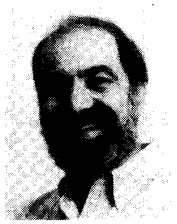

Fawwaz T. Ulaby (M'68–SM'74–F'80) received the B.S. degree in physics from the American University of Beirut, Lebanon, in 1964 and the M.S.E.E. and Ph.D. degrees in electrical engineering from the University of Texas, Austin, in 1966 and 1968, respectively.

He is currently Professor of Electrical Engineering and Computer Science at The University of Michigan, Ann Arbor, and Director of the NASA Center for Space Terahertz Technology. His current interests include microwave and millimeter wave remote sensing, radar systems, and radio wave propagation. He has authored several books and published over 400 papers and reports on these subjects.

Dr. Ulaby is the recipient of numerous awards, including the IEEE Geoscience and Remote Sensing Distinguished Achievement award in 1983, the IEEE Centennial Medal in 1984, the Kuwait Prize in applied science in 1986, and the NASA Achievement Award in 1990.